

Original Article

DOI 10.1007/s12206-020-1123-2

Keywords:

- Combined cold extrusion
- Spur gear
- Internal spline
- Tool design and fabrication
- Dimensional compatibility

Correspondence to:

Tae-Wan Ku
longtw@pusan.ac.kr

Citation:

Ku, T.-W. (2020). A combined cold extrusion for a drive shaft: experimental assessment on dimensional compatibility. *Journal of Mechanical Science and Technology* 34 (12) (2020) 5213–5222. <http://doi.org/10.1007/s12206-020-1123-2>

Received May 18th, 2020

Revised August 18th, 2020

Accepted September 20th, 2020

† Recommended by Editor
Hyung Wook Park

A combined cold extrusion for a drive shaft: experimental assessment on dimensional compatibility

Tae-Wan Ku

Engineering Research Center of Innovative Technology on Advanced Forming, Pusan National University, Busan 46241, Korea

Abstract A combined cold extrusion process is experimentally visualized to manufacture a drive shaft. Due to the requirements of a face width of about 92.00 mm for the spur gear section and a groove depth of roughly 22.70 mm for the internal spline region, a preform is adopted to prevent excessive accumulation of plastic deformation. AISI 1035 medium carbon steel material is spheroidized and annealed to use as the initial billet workpiece. In order to verify the deformed configuration and the dimensional accuracy, both shoulder angles of (θ_1 , θ_2) are selected to be (30°, 30°) and (45°, 45°) on each extrusion die for the preform forging and the combined extrusion. Using the prepared tool components, experimental investigations on the dimensional relevancy of the cold forged drive shaft are performed. When the shoulder angle set of (30°, 30°) is applied, the required dimensions with respect to the face width and the groove depth are sufficiently satisfied, but unpredictable forging defects are observed. With the shoulder angles of (45°, 45°), the drive shaft is well deformed and fabricated without any cold forging defects. As a result, it is confirmed that the drive shaft can successfully be actualized with the dimensional precision satisfied by the combined cold extrusion.

1. Introduction

As one of various metal components used in industrial hydraulic pumps, a drive shaft plays an important function in transmitting rotation power from a prime mover to an inner actuator [1, 2]. The drive shaft has an externally distinctive outline wherein an internal spline structure and a spur gear geometry are conjoined together into a single mechanical-structural part [3, 4]. The internal spline is mechanically connected to the shaft member of the prime mover, so the rotation power generated by the prime mover is directly conveyed to the drive shaft, and the transferred rotation power is simultaneously passed to the actuator of the pump through the spur gear on the drive shaft. The drive shaft used for the mechanical-structural metal member within the pumps must be guaranteed to have a precise gear shape, high wear resistance and durability, and high structural stiffness against torque [5]. In order to satisfy these requirements, inherent defects such as voids and micro-cracks, and residual stress, should be eliminated or minimized [6]. Accordingly, as an admissible production technology to manufacture the drive shaft, the metal forging process is recommended for wider usage beyond material removal and machining.

Due to the facts that the internal spline has a deep groove with an irregular hexadecagonal cross-section, and that the spur gear has a sixteen-tooth profile, and both of the geometries are merged into the drive shaft, it has proven difficult to produce this metal component through a single forging operation. When the initial billet is directly extruded to the final shape, a series of forging defects due to damage accumulation caused by excessive plastic deformation can appear. It is therefore logical to adopt an intermediate workpiece as a preform, and to apply a combined extrusion [7-9].

Regarding the prior approaches related to the drive shaft production, the two-stage cold

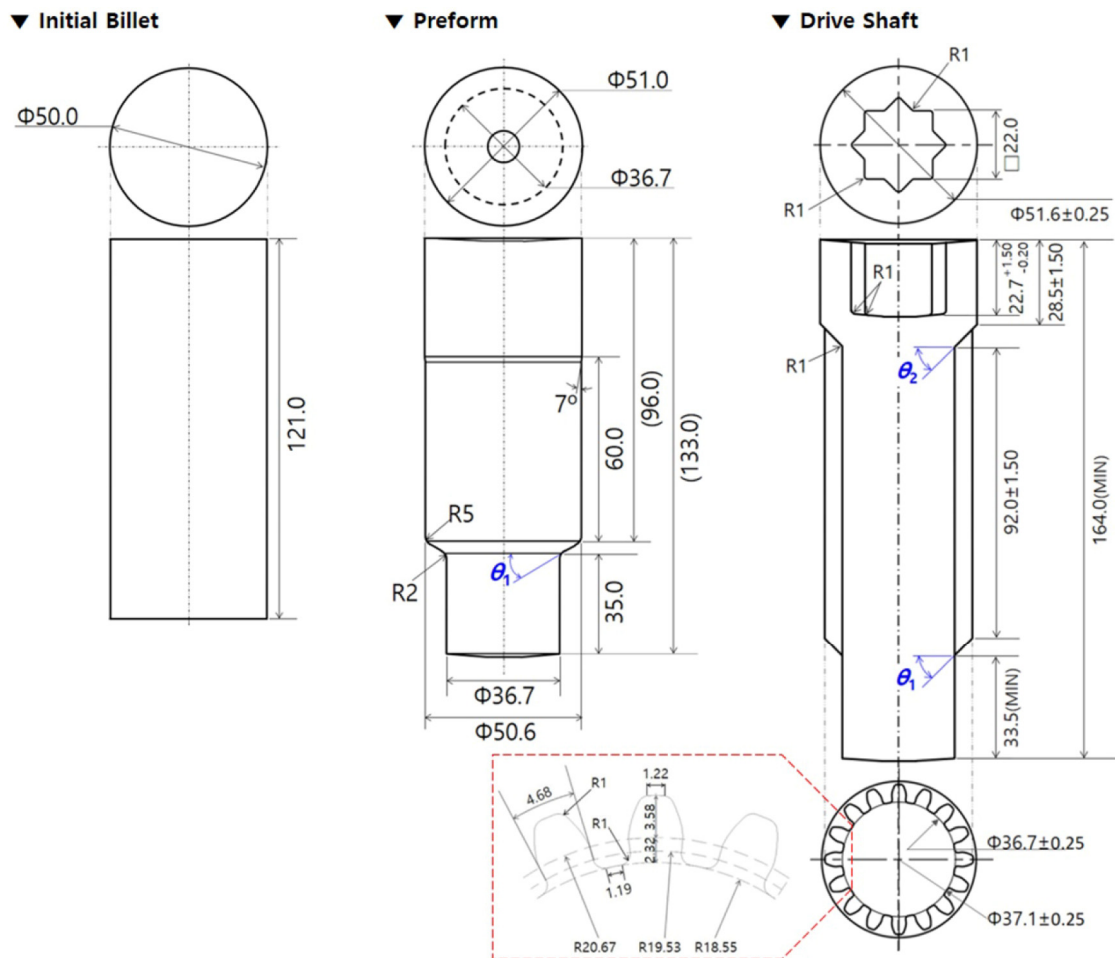


Fig. 1. Schematic views of process flow and detail dimensions for cold forging of drive shaft with shoulder angles of 45° and 45° for θ_1 and θ_2 (unit : mm).

forging operation consisting of the forward extrusion and the forward-backward one was proposed through a study on the appropriate design methodology of the preform and the initial billet, as well as the forging process [1]. As the other, FEM-based numerical simulations and the parametric evaluations to determine the proper extrusion angle combination on each die for the forward extrusion to produce the preform and for the combined one to manufacture the drive shaft were performed. The results indicated that the appropriate angles are θ_1 of 45° on the extrusion die for the preform, and θ_2 of 45° on that for the combined extrusion [2]. These numerically simulated and predicted results which obtained from the precedent parametric studies for the combined extrusion must be experimentally verified to confirm their validity.

Experimental investigations and evaluations were proceeded on the shoulder angle combination sets of $(30^\circ, 30^\circ)$ and $(45^\circ, 45^\circ)$ for (θ_1, θ_2) . As a cold drawn round bar, AISI 1035 medium carbon steel was chosen to use as the workpiece, and it was spheroidized and annealed to improve the mechanical properties and the forgeability. The experimental verifications on the dimensional relevancy of the cold forged drive shaft were carried out by using the prepared tool components. When the

shoulder angle set of $(30^\circ, 30^\circ)$ was applied as a control case, the required dimensions with respect to the face width and the groove depth were sufficiently satisfied, but unpredictable forging defects were observed. By contrast, with the shoulder angles of $(45^\circ, 45^\circ)$, the drive shaft was well deformed and fabricated without any cold forging defects. Resultantly, it was confirmed that the drive shaft can successfully be actualized with the desired dimensional precision by the combined cold extrusion.

2. Cold forging process for drive shaft

2.1 Combined cold forging process

The drive shaft that requires a total length of over 164.00 mm can be divided into three regions such as the internal spline region, the spur gear section, and the lower shaft area as shown in Fig. 1. Regarding the geometric features, the internal spline has an outer diameter of nearly 51.60 mm and the groove depth of about 22.70 mm on the irregular hexadecagonal cross-section. Also, the spur gear section has a face width of roughly 92.00 mm on the top land of the sixteen-tooth profile, and a whole depth of each tooth of 5.90 mm, and a root diame-

ter of nearly 37.10 mm. Meanwhile, the lower shaft has a length of about 33.50 mm and an outer diameter of roughly 36.70 mm.

In producing the drive shaft with three-dimensionally complicated shape, the preform forging and the combined extrusion are adopted. In detail, the initial billet with a height of 121.00 mm and a diameter of 50.00 mm is forwardly forged until the extruded length reaches about 35.00 mm, then the preform is obtained. And the combined cold extrusion, which a backward forging to shape the internal spline and a forward operation to realize the spur gear were combined into a single process, is performed.

As the forward and the combined cold extrusions are conducted successively and the whole length of the extruded workpiece is quite long, the billet material should ensure the forgeability and the ductility. Further, because the drive shaft is a torque-carrying member that conveys rotational power from a prime mover to an inner actuator within the industrial hydraulic pumps, it must provide high endurance characteristics, high corrosion and wear resistances, and high mechanical strength and structural stiffness against the torque. In an attempt to satisfy the required properties, AISI 1035 medium carbon steel was chosen as the raw workpiece material. The chemical compositions of the AISI 1035 carbon steel material are summarized in Table 1.

2.2 Mechanical properties of AISI 1035

It is common that the cold drawn carbon steel materials mostly have irregular and uneven microstructures, so it is improper to directly use any of them as the initial billet material for the cold forging operations. For this reason, the raw material was generally heat treated in order to more regularly rearrange the microstructures and to improve the mechanical properties through a spheroidizing heat treatment [10]. Thus, the spheroidizing and annealing was achieved through the temperature-time flow as presented in Fig. 2(a), and the microstructures are presented in Figs. 2(b) and (c). Then, the average grain sizes of the raw and the spheroidizing-annealed workpieces were measured to be about $8.84 \mu\text{m}$ and $9.36 \mu\text{m}$, and it was revealed that the microstructure after the heat treatment was well spheroidized as shown in Fig. 2(c).

Moreover, based on the standard specification for tensile testing of metallic materials (ASTM E8/E8M), uni-axial tensile tests were performed using the AISI 1035 specimens before and after the spheroidizing and annealing, and the measured mechanical properties are summarized in Table 2. When the initial billet was forward extruded to the preform, a series of the residual stresses are tended to inherently remain in the deformed workpiece. Also, if the residual stresses are accumulated by the following forging operations, critical defects affecting the durability and mechanical-structural performance of the final product can occur, so it is necessary to relieve the residual stresses. As one of the adequate methods to relieve the inherent residual stress without change of the microstructures and

Table 1. Chemical compositions of AISI 1035 medium carbon steel [wt%].

Elements	C	Mn	Si	P	S	Fe
As received	0.350	0.800	0.275	0.003	0.005	Bal.

Table 2. Mechanical properties of AISI 1035 workpiece material [1, 2].

Properties	Unit	Measured values by uni-axial tensile tests	
		Raw	Spheroidizing+annealing
Young's modulus	GPa	196	196
Yield strength	MPa	410	350
Ultimate strength	MPa	755	643
Poisson's ratio	-	0.29	0.29
Average grain size	μm	8.84	9.36

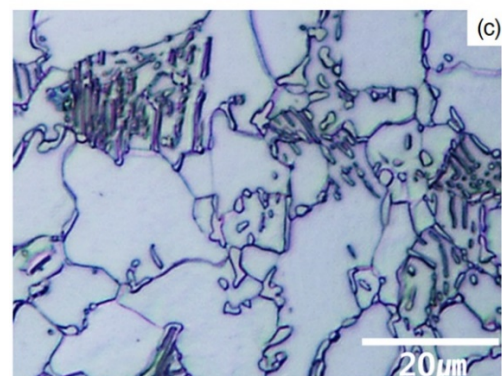
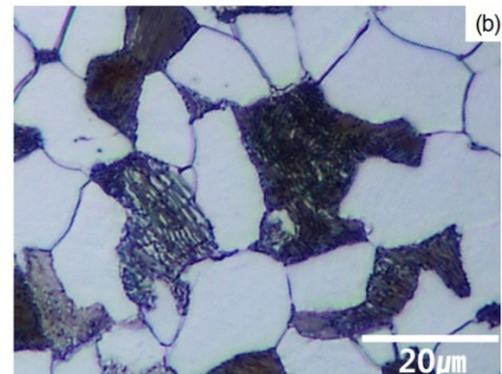
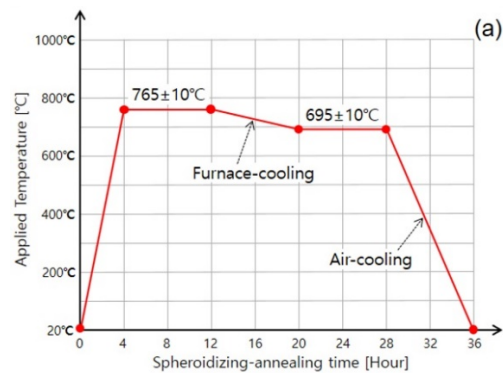


Fig. 2. Microstructures of AISI 1035 medium carbon steel: (a) temperature-time history for spheroidizing-annealing; (b) microstructures of raw workpiece; (c) microstructures of spheroidized-annealed material.

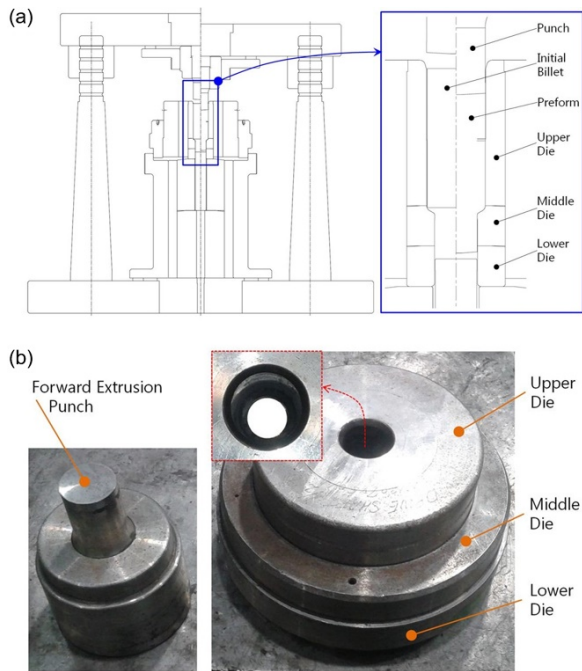


Fig. 3. Forging punch and forward extrusion die assembly for preform fabrication: (a) tool structure and its assembly; (b) fabricated forging punch and die assembly.

mechanical properties, a low temperature annealing is strongly recommended. Therefore, the low temperature annealing was considered here in order to relieve the residual stress within the forward extruded workpiece.

3. Tool design and fabrication

3.1 Forging tools for forward extrusion

Regarding the cold forging process, it is known that the tool components must be prepared with the same configurations in accordance with the results derived from the process design. In this study, the cold forging punch and the forward extrusion die assembly were considered for the preform fabrication with the detailed dimensions in Fig. 1. Here, the forward extrusion die assembly consisted of the three sub-structures of the upper and the middle, and the lower dies. In particular, because the middle die has the responsibility of realizing the preform, the shoulder angle of 45° was directly applied as the incline angle on the extrusion (middle) die. Based on the design results of the preform presented in Fig. 1, along with the tool structures as illustrated in Fig. 3(a), the tool components were fabricated using the high strength tool steel material of AISI D2 (SKD11), the hardness (H_{RC}) of which was controlled in the range of 58.0 to 60.0 by the quenching and the tempering operations [11, 12]. As this AISI D2 tool material has a tensile yield strength of about 1200 MPa and a compressive limit of nearly 2200 MPa, it was chosen with the belief that this tool material could sufficiently endure the effective stress of nearly 1000 MPa predicted from the prior numerical simulation as well as the forging load of about 250 Ton_f [2]. Fig. 3(b) shows the fabri-

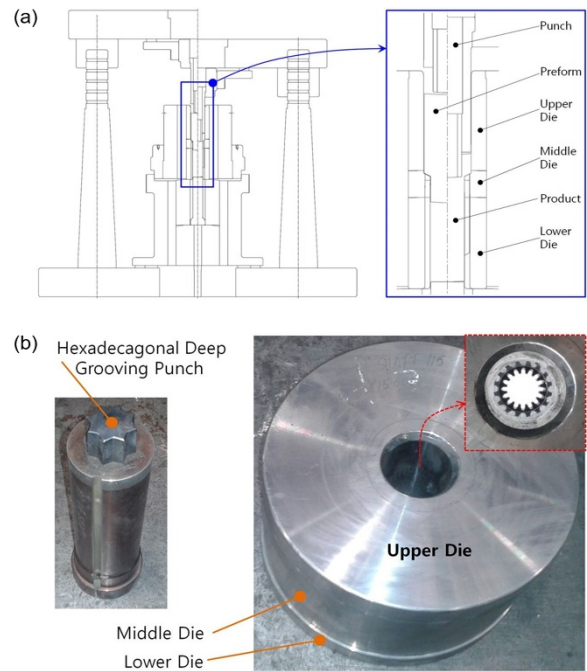


Fig. 4. Forging punch and combined extrusion die assembly for drive shaft manufacturing: (a) tool structure and its assembly; (b) fabricated forging punch and die assembly.

cated tool components such as the cold forging punch and the forward extrusion die assembly for actualizing the preform using the spheroidized-annealed AISI 1035 round billet.

3.2 Forging tools for combined extrusion

Based on the cross-sectional layout of the internal spline with a groove depth of 22.70 mm, the detailed shape of the forging punch and the die assembly was designed as shown in Fig. 4(a). The die geometries can also be visualized using the tooth profile and the shoulder angle in Fig. 1. According to these considerations, the forging punch for realizing the irregular hexadecagonal deep groove and the die assembly for featuring the sixteen-tooth spur gear geometries were fabricated as illustrated in Fig. 4(b).

Here, the extrusion die assembly was regarded to be composed of three sub-structures, which were similar to those for the preform forging. The forging tool components were manufactured using the high strength tool steel material of AISI D2 (SKD11) for the forging punch, as well as the upper and lower dies. Due to the fact that the tooth profile of the spur gear is actually formed and extruded on the extrusion (middle) die, high-level compressive stress is loaded on the middle die, which may lead to the abrasion problem of the die material. To address this, a cemented carbide alloy (D60) material with the tensile yield strength of about 3600 MPa and the compressive limit of over 5000 MPa was used to fabricate the extrusion (middle) die, then the macro hardness (H_{RC}) was controlled in the range of 60.0 to 62.0 [11, 12]. Fig. 4(b) depicts the prepared tool components for the combined cold extrusion.

4. Experimental investigations

With the results derived from the prior parametric investigation on the tool geometry for fabricating the drive shaft [2], when the shoulder angles of (θ_1, θ_2) were set to be $(45^\circ, 45^\circ)$, it was shown that the drive shaft could be well visualized by the combined cold extrusion. However, it was necessary to check whether or not the excessive sinking and the defect of the tooth shape have actually occurring. As a representative comparison target in the geometric parameters, the shoulder angle set of $(30^\circ, 30^\circ)$ was selected to demonstrate the suitability in terms of the selection of the applicable process parameter. For the preliminary experiments, the extrusion (middle) dies to fabricate the preform and the drive shaft were separately prepared with each shoulder angle of 30° and then the forward and the combined operations were progressively tested. In all experimental investigations, a phosphophyllite coating on the outer surfaces of AISI 1035 initial billet with a diameter of 50.00 mm and a height of 121.00 mm was applied to ensure a low-level frictional resistance on the contact interfaces between the workpiece and the cold forging tools [5].

4.1 Preliminary experiment

The preliminary prototyped drive shaft is presented in Fig. 5, where it can be seen that the internal spline part was backwardly well forged, and that the spur gear part was forwardly shaped. However, a series of the cold forging defects were observed around the shoulder region where the spur gear part and the internal spline section meet, and excessive sinking also occurred on the center area of the internal spline part. This sinking phenomenon had already been predicted [2], but the cold forging defects leading to the unevenly agglomerated workpiece material was not foreseen. The local agglomeration was attributed to the fact that small amounts of the squeezed materials converged upon the shoulder area when the preform was extruded by the combined cold forging. The other issue was attributed to the inadequate shoulder angle on the extrusion die, because the internal spline and the spur gear geometries were well shaped. Consequently, it was demonstrated that the results of the preliminary experiment on the shoulder angles of $(30^\circ, 30^\circ)$ were consistent with those of the prior approaches [1, 2].

4.2 Forward extrusion for preform

Based on the evidence obtained from the preliminary experiment, the numerically predicted results as summarized in the prior study were verified [2], and it was also confirmed that the shoulder angle set of $(\theta_1 = 45^\circ, \theta_2 = 45^\circ)$ leads to the applicable geometric parameters for realizing the required configurations and dimensions as outlined in Fig. 1. Accordingly, the shoulder angle of 45° was adopted on the extrusion (middle) die to produce the preform, and the spheroidized and annealed round billet with a diameter of 50.0 mm and a length of

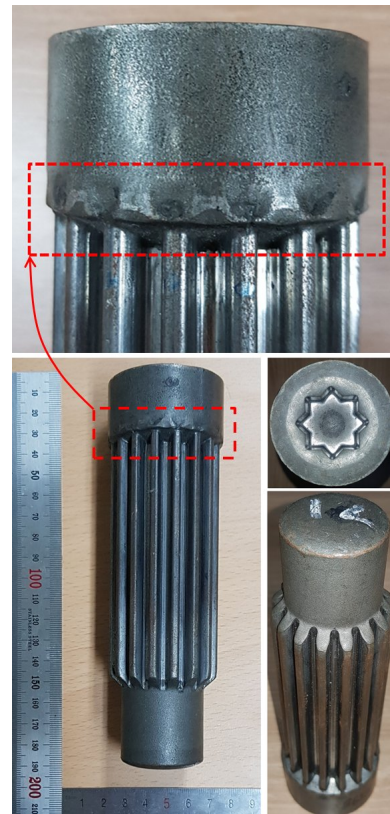


Fig. 5. Preliminary fabricated drive shaft with cold forging defects.

121.0 mm was used for the initial workpiece. The forging press with the capacity of 600 Ton_r was used to fabricate the preform through the forward extrusion process. Fig. 6(a) depicts that the preform fabricated through the forward cold extrusion, and it appears to have been externally well featured. Regarding the detailed dimensions of the forward extruded preform, it had the outer diameters of about 51.02 mm for the upper head part, of nearly 50.64 mm for the middle shaft one, of roughly 36.71 mm for the lower shaft, and the total length was approximately 135.41 mm. The measured values matched the specifications of the preform described in Fig. 1, very well.

4.3 Combined extrusion for drive shaft

During the combined (forward-backward) cold extrusion operation, in order to avoid excessive accumulation of the inherent residual stress within the preform, the low temperature annealing was first pursued for 3 hours at $700^\circ\text{C} \pm 10^\circ\text{C}$ and about 30 hours at room temperature of about 20°C . The preform which was relieved the residual stress was then applied to the combined extrusion experiments. The cold forging tool set illustrated in Fig. 4(b) was directly accepted for prototyping the drive shaft. As the tooth profile of the spur gear is formed and forwardly protruded on the extrusion (middle) die, at the same time, that the irregular hexadecagonal deep groove is backwardly extruded, the slope angle (θ_2) of the extrusion (middle) die was determined to be 45° , and this angle was adopted to

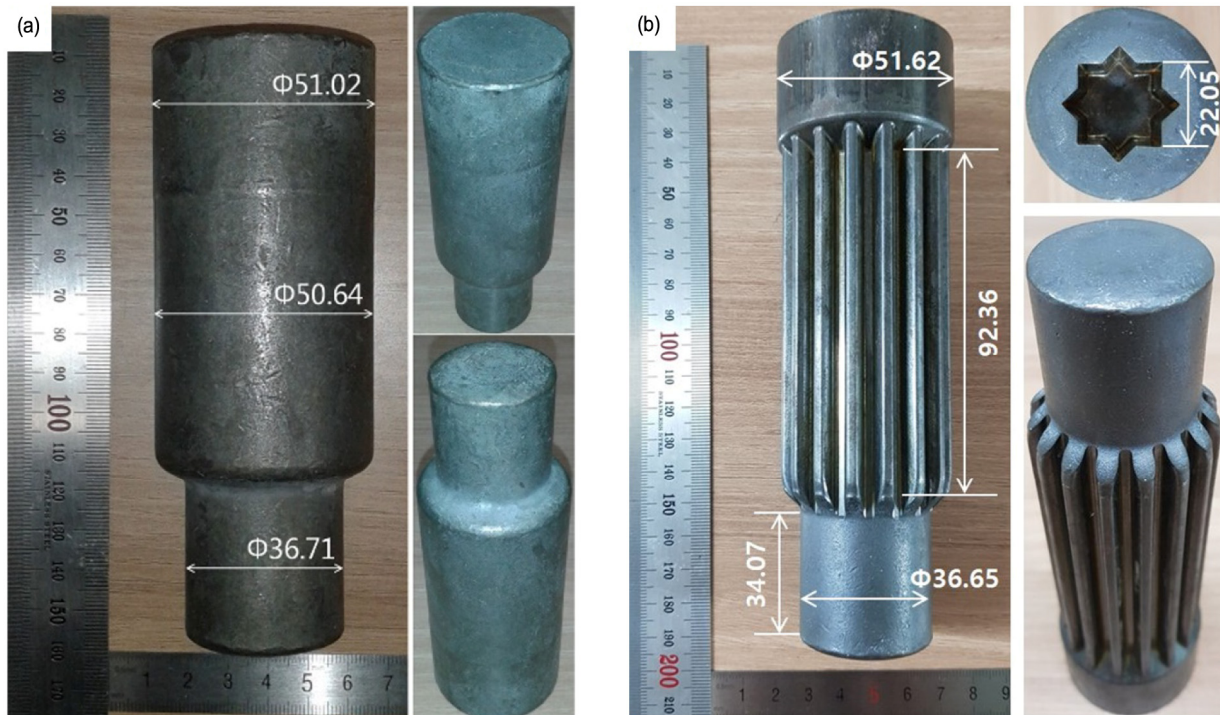


Fig. 6. Cold forged prototypes (unit : mm): (a) preform by forward extrusion; (b) drive shaft by combined extrusion.

the fabrication of the extrusion (middle) die for manufacturing the drive shaft. The cold forging press with a capacity of 600 Ton_f was used for the combined cold extrusion experiments.

Using the preform that the residual stress was relieved by the low-temperature annealing, as well as the prepared tool components, the combined cold extrusion experiments were carried out, and Fig. 6(b) presents the deformed drive shaft. Regarding the simply and manually measured dimensions, the outer diameter of the internal spline part was nearly 51.62 mm, that of the lower shaft was roughly 36.65 mm, the face width of the spur gear was approximately 92.36 mm, and the extruded length of the lower shaft was about 34.07 mm. Even when considering the error range associated with the easily measured dimensions by a vernier caliper, it was revealed that the obtained values satisfied the specifications of the drive shaft shown in Fig. 1.

5. Results and discussions

For evaluating the dimensional compatibility, the preform in Fig. 6(a) and the drive shaft in Fig. 6(b) were fully captured using an optical 3D scanner with feature and surface noise vibration under 10 μm . Fig. 7(a) shows the 3D scanned feature of the preform, and Fig. 7(b) presents the fully captured shape of the drive shaft. In Fig. 7(b), it can be seen that a series of optical scanning noises were locally detected around the bottom land on the spur gear and the grooved corner in the upper head part. This scanning noise was attributed to the interference of the irradiated light source that occurs due to the relatively narrow and deep features compared to the overall

shape of the drive shaft. Despite these facts, the 3D captured configurations of the cold forged preform and the cold extruded drive shaft were regarded to be accurate with the consideration that the dimensional variation derived from the scanning noise may be not severe. The 3D scanned images were used to compare the dimensional relevance with the designed shapes. For evaluating the geometric compatibility of the prototyped preform and the fabricated drive shaft, an image processing software (Geomagic Qualify) was used for figuring out the relatively geometric variation between the comparable objects.

5.1 Dimensional accuracy of preform

Fig. 8 illustrates the compared results in accordance with the one-sixteenth model of the preform. In detail, Fig. 8(a) indicates the result of the comparative investigation with regard to the dimensional variation between the designed target preform and the 3D scanned feature, while Fig. 8(b) shows that between the captured feature and the numerically predicted configuration. Here, the numerically simulated feature of the preform was sourced from the prior obtained results on the parametric study related to this combined extrusion [1, 2]. Overall, it was observed that the dimensional differences were sufficiently small and fell within the error range of -0.25 mm to 0.25 mm.

By contrast, the distinctive deformation behavior was clearly observed around the extruded end of the lower shaft. It can be described that the workpiece at the center region of the lower shaft was relatively more extruded than that around the external part, which was attributed to the frictional characteristics between the die surfaces and the workpiece. For this reason,

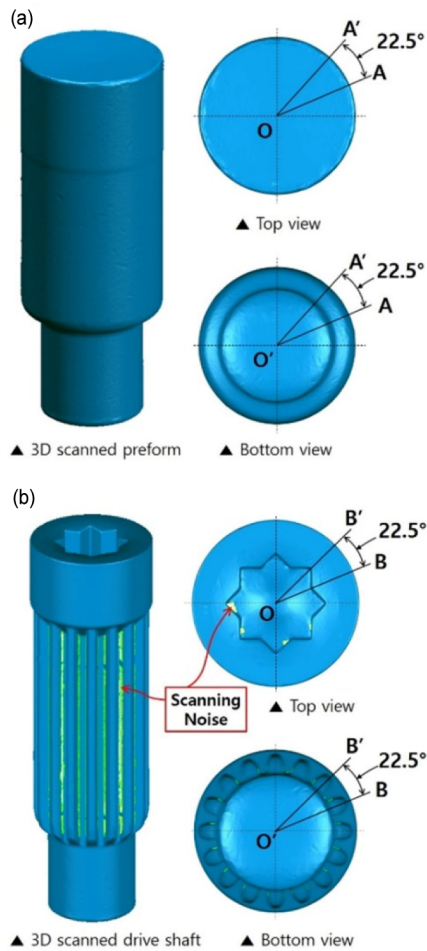


Fig. 7. (a) 3D scanned preform; (b) fully captured drive shaft.

the experimentally fabricated preform by the cold forward extrusion was more protruded with approximately 3.75 mm around the end region and with roughly 3.55 mm at the end part than the designed target geometry on the center area of the lower shaft, as presented in Fig. 8(a).

When comparing the fully scanned image with the preform configuration predicted by the prior parametric investigations [2], despite the similarity of the deformation behavior due to the variation of the relative extrusion velocity induced by the difference in frictional behavior at each region, it was revealed that the dimensional error in the variation range of -0.20 mm to 1.15 mm was slightly decreased roughly 2.50 mm as shown in Fig. 8(b).

5.2 Dimensional relevancy of drive shaft

The dimensional error of the drive shaft actualized through the combined cold extrusion experiment was compared with the designed target shape as illustrated in Fig. 9. Overall, it was evaluated that the variations were small and consistent with the error range of -0.25 mm to 0.25 mm. In Fig. 9, the shape errors induced from the scanning noise were campily

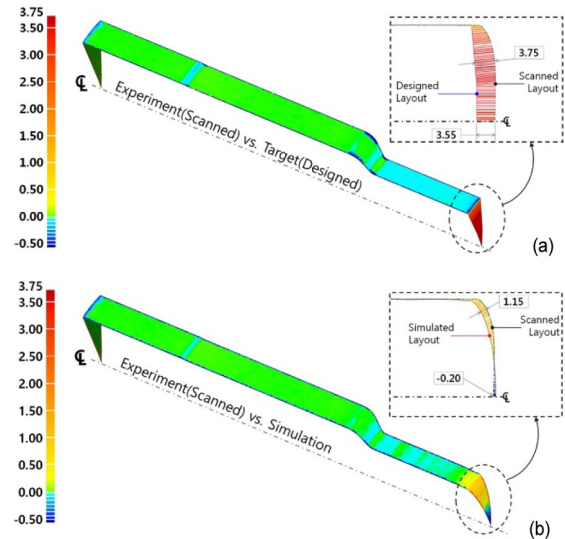


Fig. 8. Comparison results on dimensional error among 3D captured image and designed shape and numerically predicted geometry of preform (unit: mm): (a) 3D scanned image vs. designed shape; (b) 3D scanned image vs. numerically predicted geometry [2].

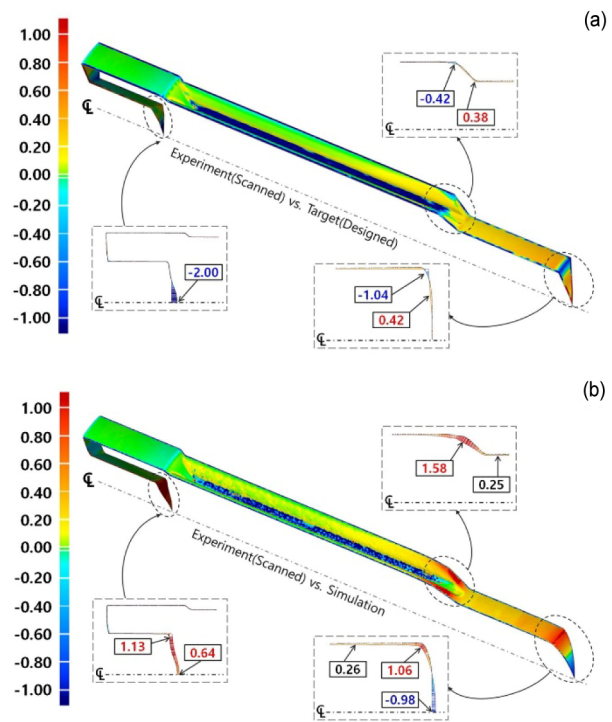


Fig. 9. Comparison results on dimensional variation among 3D captured image and designed shape and numerically predicted geometry of drive shaft (unit: mm): (a) 3D scanned image vs. designed shape; (b) 3D scanned image vs. numerically predicted geometry [2].

presented. Aside from the sections being affected by the scanning noise, the dimensional suitability of the drive shaft was investigated. Regarding the locally distributed difference contour shown in Fig. 9(a), a sinking depth of about -2.00 mm in

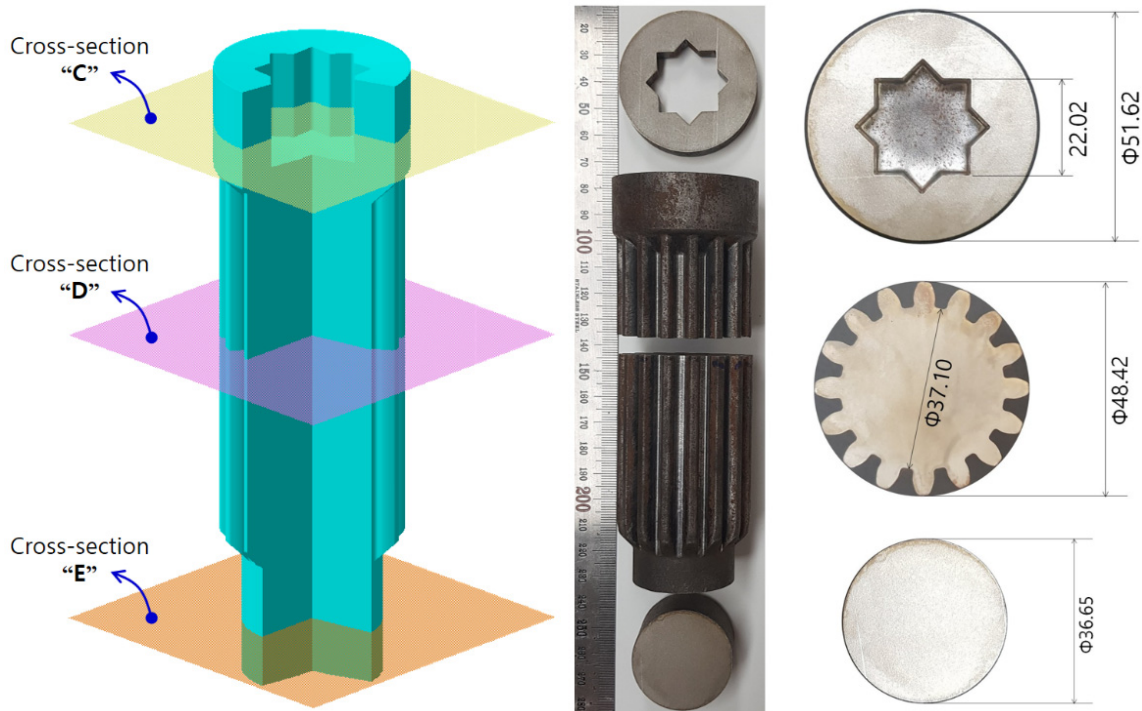


Fig. 10. Cross-sectional dimensions of drive shaft fabricated through combined cold extrusion (unit : mm).

the upper head region (that is, at the deep grooved bottom area) of the experimentally prototyped drive shaft was observed. Further, the shape error of roughly -1.04 mm at the end tip region of the lower shaft was observed, but that around the tooth end of the spur gear was distributed as a small value in the range of -0.42 mm to 0.38 mm.

In addition, Fig. 9(b) displays the distribution of the dimensional error between the 3D scanned image and the simulated drive shaft. Here, the numerically simulated feature of the pre-form was sourced from the result obtained from a previous parametric study related to this combined extrusion [2]. The error at the hexadecagonal deep grooved bottom section was gauged to be in the range of 0.64 mm to 1.13 mm, while that on the end of the lower shaft was estimated with the limits of -0.98 mm to 1.06 mm, and that around the extrusion end of the spur gear was measured with the scope of about 1.58 mm. Remarkably, it was shown that the dimensional variation contours in Fig. 9 differed only slightly from the required values as the vertical distance.

Due to the fact that the image processing software presents the relative distance between the comparative objects, these error distributions can be explained. In order to ensure the geometric relevance of the cold forged drive shaft, the dimensions of the main features were measured using a digital vernier caliper with a resolution of $10 \mu\text{m}$. As shown in Fig. 10, the drive shaft was cut into four pieces with three cross-sectional planes denoted as C, D, and E. In the cross-section C at the internal spline region, the width of the deep groove was measured as 22.02 mm, while the outer diameter was 51.62 mm. The root diameter of the spur gear geometry in the

cross-section D was gauged at 37.10 mm, while the tooth height was 5.66 mm. In addition, the outer diameter of the lower shaft was investigated with the value of 36.65 mm as displayed in the cross-section E.

5.3 Metal flow of cold forged drive shaft

During the combined cold extrusion, it is important that the metal flow lines (or the grain flow lines) in the drive shaft form in the proper direction, because the forward and the backward extrusions are simultaneously operated. In order to visualize the metal flow lines and ensure the adequacy of the sequential cold forging processes proposed in this study, the drive shaft manufactured through the combined cold extrusion was cut along the longitudinal direction. Then the corrosion tests on the cross-section of the longitudinally cut specimen were performed. On the whole, it was noticed that the metal flow lines were well distributed as shown in Fig. 11.

In particular, the metal flows around the upper head region (Sec. 1) that the workpiece extrudes in opposite (forward and backward) directions were observed to be suitably formed without the discontinuity and the overlap, as well as around the end (Sec. 3) of the forwardly extruded tooth of the spur gear. Especially, it was verified that the metal flow lines in Sec. 2 (that is, the sinking area predicted in the numerical simulations and observed in the experimental investigations) were appeared symmetrically without any broken. Based on these metal flow lines, it was ensured that the drive shaft can be successfully fabricated through the combined cold extrusion process.

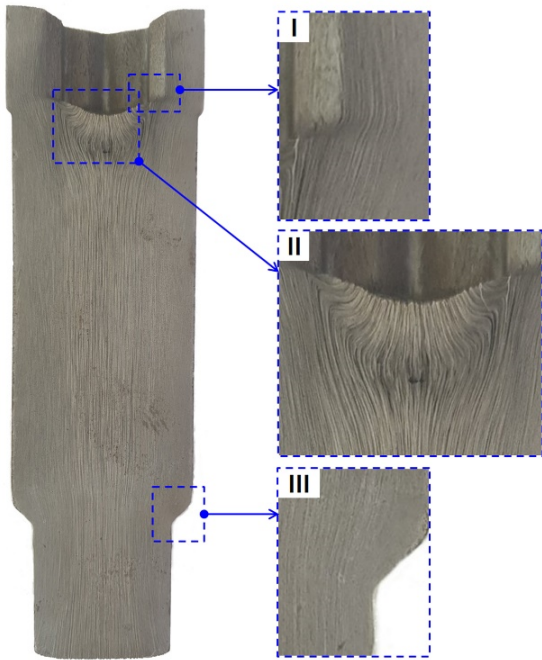


Fig. 11. Metal flow of cold forged drive shaft.

6. Conclusions

In this study, the combined cold extrusion for fabricating a drive shaft used for the industrial hydraulic pumps was experimentally investigated. The external layout of the drive shaft had a distinct configuration of the lower shaft and the sixteen-tooth spur gear, as well as the irregularly deep grooved internal spline. AISI 1035 medium carbon steel material was first spheroidized and annealed to improve and re-arrange the microstructures. In addition, the preform by the forward extrusion operation was re-annealed using the low temperature annealing for eliminating the residual stress induced from the forward extrusion. Then, the combined cold extrusion process was experimentally realized. The fabricated preform and the produced drive shaft were fully scanned using an optical 3D scanner, so that the captured features could be compared with the demanded geometries. The results achieved through the experimental verifications can be summarized as follows;

(1) In order to investigate the microstructure and the grain size of the AISI 1035 billet workpiece, the spheroidizing and annealing was pursued for 4 hours at $765\text{ }^{\circ}\text{C} \pm 10\text{ }^{\circ}\text{C}$ and for 8 hours at $695\text{ }^{\circ}\text{C} \pm 10\text{ }^{\circ}\text{C}$, then the microstructures were observed to be well spheroidized and the initial grain size of about $8.84\text{ }\mu\text{m}$ was slightly increased to nearly $9.36\text{ }\mu\text{m}$.

(2) The spheroidized and annealed AISI 1035 initial round billet was forwardly extruded to realize the preform. The low-temperature annealing for 3 hours at $700\text{ }^{\circ}\text{C} \pm 10\text{ }^{\circ}\text{C}$ and 30 hours at room temperature of about $20\text{ }^{\circ}\text{C}$ was carried out for eliminating the potentially inherent residual stresses in the cold forged preform, and the re-annealed preform was applied to the drive shaft production by the combined cold extrusion operation.

(3) When the shoulder angle set of $(30^{\circ}, 30^{\circ})$ as a control case was adopted, the cold forging defects induced from the unevenly agglomerate workpiece materials around the shoulder area of the cold forged drive shaft were observed. However, when the combination of $(45^{\circ}, 45^{\circ})$ was applied, these defects did not occur.

(4) A series of comparative evaluations on the dimensional accuracy on the cold forged preform and the cold extruded drive shaft without any cold forging defects were performed, and the results verified that these dimensional variations were each well within the permissible error ranges.

(5) Resultantly, it was confirmed that the drive shaft with the spur gear and the internal spline geometries can be actually realized through the preform forging and the combined cold extrusion with the dimensional compatibility.

Acknowledgments

This work was supported by the Engineering Research Center Program (NRF-2019R1A5A6099595) and the Basic Science Research Program (NRF-2017R1D1A1B03032741) through the National Research Foundation of Korea (NRF) grant funded by the Korea government.

References

- [1] T. W. Ku, A study on two-stage cold forging for a drive shaft with internal spline and spur gear geometries, *Metals*, 8 (11) (2018) 953.
- [2] T. W. Ku, A combined cold extrusion for a drive shaft : a parametric study on tool geometry, *Materials*, 13 (10) (2020) 2244.
- [3] J. H. Song and Y. T. Im, The applicability of process design system for forward extrusion of spur gears, *Journal of Materials Processing Technology*, 184 (1-3) (2007) 411-419.
- [4] T. Maeno, K. Mori, Y. Ichikawa and M. Sugawara, Use of liquid lubricant for backward extrusion of cup with internal spline using pulsating motion, *Journal of Materials Processing Technology*, 244 (2017) 273-283.
- [5] T. W. Ku and B. S. Kang, Tool design for inner race cold forging with skew-type cross ball grooves, *Journal of Materials Processing Technology*, 214 (8) (2014) 1482-1502.
- [6] S. Brunbauer, G. Winter, T. Antretter, P. Staron and W. Ecker, Residual stress and microstructure evolution in steel tubes for different cooling conditions – simulation and verification, *Materials Science and Engineering : A*, 747 (2019) 73-79.
- [7] M. Sedighi and S. Tokmechi, A new approach to preform design in forging process of complex parts, *Journal of Materials Processing Technology*, 197 (1-3) (2008) 314-324.
- [8] T. W. Ku, L. H. Lee and B. S. Kang, Multi-stage cold forging and experimental investigation for the outer race of constant velocity joints, *Materials and Design*, 49 (2013) 368-385.
- [9] M. S. Joun, J. H. Chung and R. Shivpuri, An axisymmetric forging approach to preform design in ring rolling using a rigid-viscoplastic finite element method, *International Journal of Machine Tools and Manufacture*, 38 (10-11) (1998) 1183-1191.

- [10] J. M. O'Brien and W. F. Hosford, Spheroidization cycles for medium carbon steels, *Metallurgical and Materials Transactions A*, 33 (4) (2002) 1255-1261.
- [11] T. W. Ku and B. S. Kang, Tool design and experimental verification for multi-stage cold forging process of the outer race, *International Journal of Precision Engineering and Manufacturing*, 15 (9) (2014) 1995-2004.
- [12] T. W. Ku and B. S. Kang, Hardness-controlled tool fabrication and application to cold forging of inner race with skewed ball grooves, *The International Journal of Advanced Manufacturing Technology*, 74 (9-12) (2014) 1337-1354.



Tae-Wan Ku is a Professor of the Engineering Research Center of Innovative Technology on Advanced Forming, and Department of Green Transportation System Design at Pusan National University, Busan, Republic of Korea. He received his Ph.D. in Aerospace Engineering from Pusan National University.

His research interests include multi-stage metal forming, smart forming process, process design and simplification, and applications to the manufacturing fields.